


## ORIGINAL ARTICLE

# ALDH1A3-mTOR axis as a therapeutic target for anticancer drug-tolerant persister cells in gastric cancer

Ryuhei Kawakami<sup>1,2</sup> | Tetsuo Mashima<sup>1</sup> | Naomi Kawata<sup>1,3</sup> | Koshi Kumagai<sup>4</sup> |  
Toshiro Migita<sup>1</sup> | Takeshi Sano<sup>4</sup> | Nobuyuki Mizunuma<sup>3</sup> | Kensei Yamaguchi<sup>3</sup> |  
Hiroyuki Seimiya<sup>1,2</sup> 

<sup>1</sup>Division of Molecular Biotherapy, Cancer Chemotherapy Center, Japanese Foundation for Cancer Research, Tokyo, Japan

<sup>2</sup>Department of Computational Biology and Medical Sciences, Graduate School of Frontier Sciences, The University of Tokyo, Tokyo, Japan

<sup>3</sup>Gastroenterological Medicine, Cancer Institute Hospital, Japanese Foundation for Cancer Research, Tokyo, Japan

<sup>4</sup>Gastroenterological Surgery, Cancer Institute Hospital, Japanese Foundation for Cancer Research, Tokyo, Japan

## Correspondence

Hiroyuki Seimiya, Division of Molecular Biotherapy, Cancer Chemotherapy Center, Japanese Foundation for Cancer Research, 3-8-31 Ariake, Koto-ku, Tokyo 135-8550, Japan.  
Email: hseimiya@jfccr.or.jp

## Funding information

Japan Society for the Promotion of Science, Grant/Award Number: 18H04633 and 18K07337; The Nippon Foundation, Grant/Award Number: N/A

## Abstract

Tumors consist of heterogeneous cell populations that contain cancer cell subpopulations with anticancer drug-resistant properties called “persister” cells. While this early-phase drug tolerance is known to be related to the stem cell-like characteristic of persister cells, how the stem cell-related pathways contribute to drug resistance has remained elusive. Here, we conducted a single-cell analysis based on the stem cell lineage-related and gastric cell lineage-related gene expression in patient-derived gastric cancer cell models. The analyses revealed that 5-fluorouracil (5-FU) induces a dynamic change in the cell heterogeneity. In particular, cells highly expressing stem cell-related genes were enriched in the residual cancer cells after 5-FU treatment. Subsequent functional screening identified aldehyde dehydrogenase 1A3 (ALDH1A3) as a specific marker and potential therapeutic target of persister cells. ALDH1A3 was selectively overexpressed among the ALDH isozymes after treatment with 5-FU or SN38, a DNA topoisomerase I inhibitor. Attenuation of ALDH1A3 expression by RNA interference significantly suppressed cell proliferation, reduced the number of persister cells after anticancer drug treatment and interfered with tumor growth in a mouse xenograft model. Mechanistically, ALDH1A3 depletion affected gene expression of the mammalian target of rapamycin (mTOR) cell survival pathway, which coincided with a decrease in the activating phosphorylation of S6 kinase. Temsirolimus, an mTOR inhibitor, reduced the number of 5FU-tolerant persister cells. High ALDH1A3 expression correlated with worse prognosis of gastric cancer patients. These observations indicate that the ALDH1A3-mTOR axis could be a novel therapeutic target to eradicate drug-tolerant gastric cancer cells.

## KEYWORDS

ALDH1A3, drug tolerance, gastric cancer, persister cells, tumor heterogeneity

This is an open access article under the terms of the Creative Commons Attribution-NonCommercial License, which permits use, distribution and reproduction in any medium, provided the original work is properly cited and is not used for commercial purposes.

© 2020 The Authors. *Cancer Science* published by John Wiley & Sons Australia, Ltd on behalf of Japanese Cancer Association.

## 1 | INTRODUCTION

Gastric cancer was the fifth most common and the third deadliest cancer worldwide in 2018 (<http://gco.iarc.fr/>), and its occurrence rate is particularly high in Asia.<sup>1</sup> While chemotherapeutic drugs are available for the treatment of advanced and recurrent gastric cancer, their effectiveness is limited. One striking feature of gastric cancer is that it consists of highly heterogeneous tumor tissues. Tumor heterogeneity has been postulated to be related to disease malignancy.<sup>2,3</sup> Recent reports suggest that solid tumors contain persister cells, subpopulations of drug-tolerant cancer cells that survive after chemotherapy and contribute to tumor recurrence.<sup>4,5</sup> However, the detailed characteristics and therapeutic target molecules of persister cells remain elusive.

Heterogeneous tumor tissues may contain cancer stem cells, a cell subpopulation that exhibits high tumorigenicity, multipotency and self-renewal potential.<sup>6-8</sup> In gastric cancer, the transmembrane protein CD44 and its splicing variants (CD44v) have been reported to be cancer stem cell markers.<sup>9,10</sup> Mechanistically, CD44v interacts with the glutamate-cystine transporter xCT at the cell membrane, which increases the level of reduced glutathione and confers resistance to oxidative stress.<sup>11</sup> Consistent with these reports, we used gastric cancer patient-derived cell models to show that the residual cancer cells that survived after treatment with cytotoxic anticancer drugs overexpress CD44v, and ectopic overexpression of CD44v contributes to the anticancer drug resistance.<sup>12</sup> However, to what extent these or other stem cell-like cancer cells could be involved in the early phase of drug resistance remains unknown.

Normal gastric tissue consists of various cell types that are differentiated from stem cells into progenitor cells and then surface mucous (pit), mucous gland (neck) and endocrine cells through multiple steps.<sup>13-15</sup> Recent studies have revealed the gastric cell lineage and specific markers for each cell type (summarized in Figure 1A).<sup>13-19</sup> For example, LGR5 and TROY are gastric stem cell markers, whereas SOX9 is a progenitor cell marker. MUC5AC, TFF1 and GKN1 mark pit cells, whereas MUC6 and TFF2 are hallmarks of neck cells. Considering the cell diversity and hierarchy in normal gastric tissues, cancer cells in gastric cancer tissues arising from these cells could also possess the cell diversity and hierarchy.

Single-cell analysis is a recently developed systematic method used to evaluate the heterogeneity of a cell population.<sup>20,21</sup> In the

present study, we used single-cell gene expression analysis on stem cell- and gastric cell lineage-markers and evaluated features of drug-tolerant persister cells in gastric cancer patient-derived cells (PDC). Through this analysis, we identified a potential therapeutic target pathway of gastric cancer persister cells.

## 2 | MATERIALS AND METHODS

### 2.1 | Cell culture and chemicals

Human gastric cancer PDC, JSC15-3, JSC17-2 and JSC17-7, were established with approval from the Institutional Review Board of the Japanese Foundation for Cancer Research and with informed consent from the patients as described previously.<sup>12</sup> JSC15-3 and JSC17-2 cells were cultured in ACL4/F12 (1:1) medium (Nacalai Tesque) supplemented with 5% heat-inactivated FBS and 100 µg/mL kanamycin (Meiji Seika Pharma). JSC17-7 cells were cultured in ACL4/RPMI (1:1) medium supplemented with 5% heat-inactivated FBS and 100 µg/mL kanamycin. 5-fluorouracil (5-FU), SN38, paclitaxel and temsirolimus were purchased from Sigma-Aldrich. Cisplatin was purchased from Enzo Biochem.

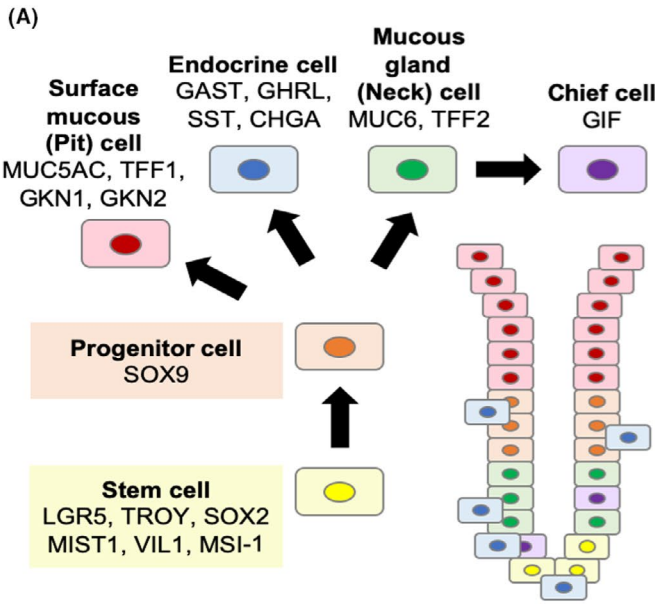
### 2.2 | Cell proliferation assay

Cells were seeded in 96-well microplates, cultured overnight and then treated with drugs for 7 days. MTT (Nacalai Tesque) was added to cells at the final concentration of 0.8 mg/mL and cells were incubated for 4 hours. The formazan was dissolved in DMSO and the optical densities at 570 and 630 nm were measured using an xMark microplate spectrophotometer (Bio-Rad). Cell proliferation was also assessed using the Cell Titer 96 Aqueous One Solution Cell Proliferation Assay Kit (Promega).

### 2.3 | Colony formation assay

Cells were seeded in 12-well collagen-coated plates in the presence of test compounds or DMSO alone and cultured for 14 days. Cells were then fixed with 10% formaldehyde (Muto Pure Chemicals) and stained with 0.5% crystal violet/ethanol (Nacalai Tesque). Each

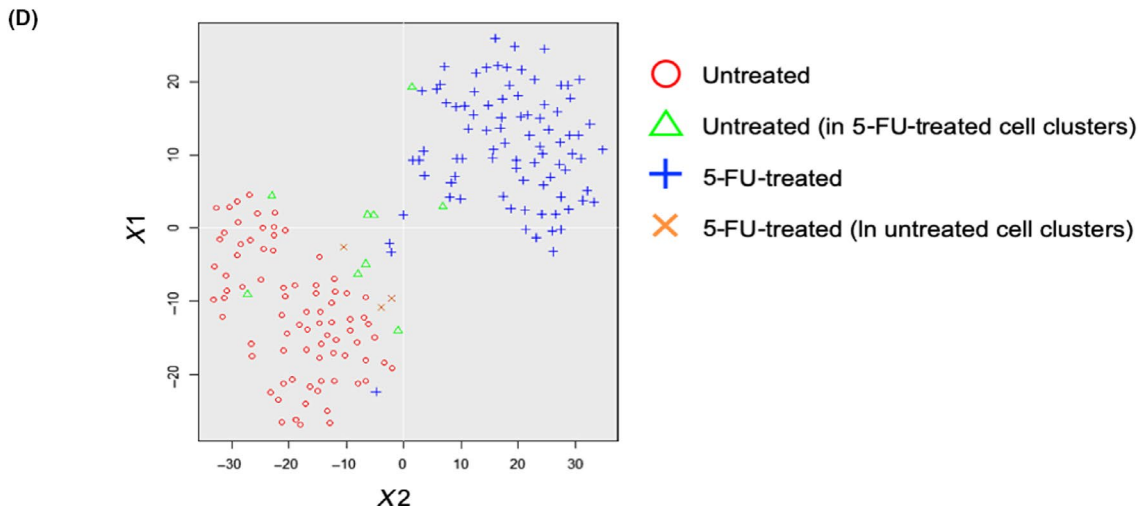
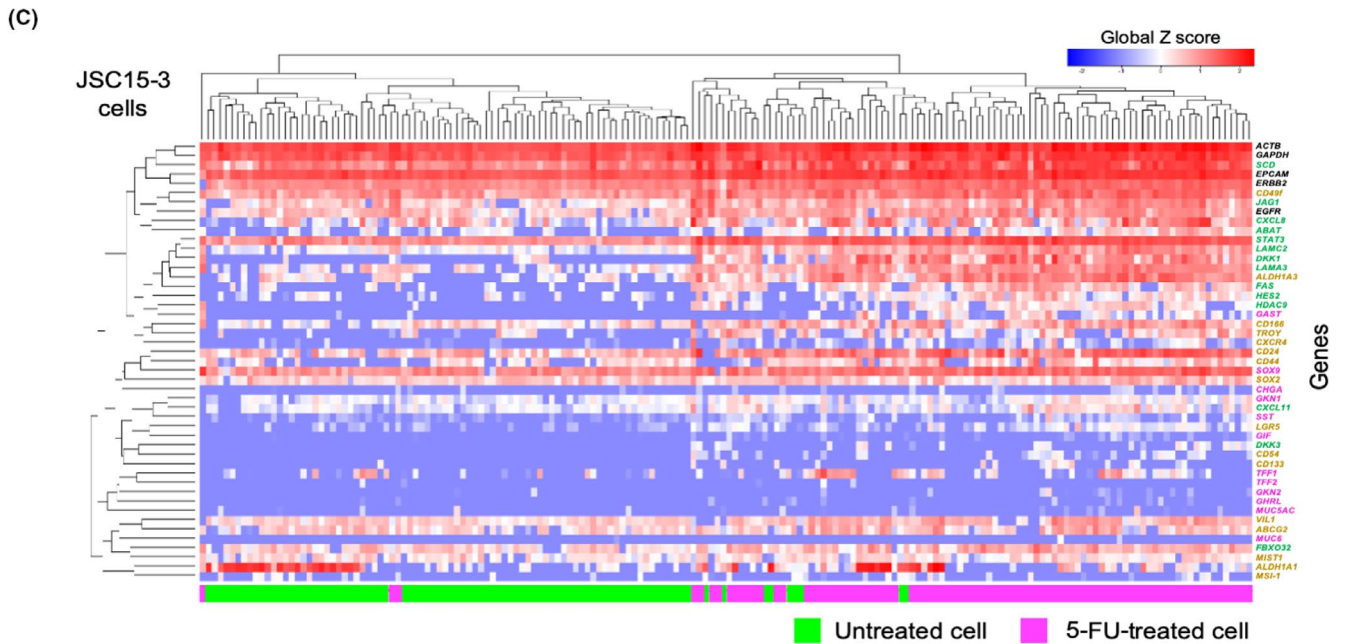
**FIGURE 1** Single-cell analysis of gastric cancer patient-derived cells reveals 5-fluorouracil (5-FU)-mediated alteration of cell heterogeneity and outlier cells. A, Schematic diagram of lineages in gastric normal tissue. The gastric cells shown on the top are differentiated, while the cells on the bottom of the schematic are undifferentiated. Representative markers of each cell used in the single-cell analysis are indicated. B, Identification of the persister-related genes. Cells were treated with the indicated drugs and subjected to GeneChip microarray analysis. Values indicate the fold induction of the gene in the drug-treated persister cells. C, Hierarchical clustering of the single-cell gene expression data in JSC15-3 cells untreated or treated with 5-FU based on the gene list in Table S3. Vertical axis: gene. Horizontal axis: cell. Green line and pink line indicate the untreated cells and 5-FU-treated cells, respectively. D, t-Distributed stochastic neighbor embedding (tSNE) analysis with the single-cell analysis data in (C). Red, light green, blue and brown indicate the untreated cells, the untreated cells in 5-FU-treated cells clusters, 5-FU-treated cells and 5-FU-treated cells in untreated cell clusters, respectively. In (C) and (D), the cells were treated with 5-FU for 7 days followed by an additional 4 days without the drug to minimize the contribution of transient drug-induced gene expression



(B)

	JSC15-3 5-FU	JSC15-3 SN38	JSC17-2 5-FU
<i>DKK1</i>	3.3	2.1	4.2
<i>STAT3</i>	2.6	1.8	2.1
<i>LAMA3</i>	4.0	1.9	3.3
<i>CXCL8</i>	3.3	2.4	3.0
<i>SCD</i>	2.4	2.3	1.5
<i>ABAT</i>	3.3	2.2	1.7
<i>DKK3</i>	4.0	4.1	2.1
<i>HDAC9</i>	4.4	2.0	3.9
<i>FAS</i>	7.5	3.2	3.7
<i>FBXO32</i>	6.8	3.6	2.4
<i>CXCL11</i>	6.3	4.6	2.4
<i>LAMC2</i>	3.4	2.7	1.9
<i>HES2</i>	2.5	1.7	3.0
<i>JAG1</i>	2.1	1.5	1.6

Fold change



well was washed with water, and the number and area of the colonies were quantitated using ImageJ software (National Institute of Health).

## 2.4 | Reverse transcription-quantitative PCR

Total RNA was extracted using the RNeasy Mini Kit (Qiagen) or the FastGene RNA Basic Kit (Nippon Genetics). cDNA was synthesized using ReverTra Ace qPCR RT Master Mix (Toyobo). Quantitative PCR (qPCR) was performed with the Power SYBR Green PCR Master Mix (Applied Biosystems) and detected using a LightCycler 96 (Roche). *Glyceraldehyde-3-phosphate dehydrogenase (GAPDH)* or  $\beta$ -actin (*ACTB*) genes were used as controls to normalize the data. PCR primers were designed by Roche primer design site or primer blast (<https://www.ncbi.nlm.nih.gov/tools/primer-blast/>), except for *GAST*, *MIST1* and *SOX2*, which were previously described.<sup>14</sup> Primer sequences are listed in Tables S1 and S2.

## 2.5 | cDNA microarray and data analysis

Total RNA was quantified using the Agilent 2100 Bioanalyzer (Agilent Technologies). cDNA microarray analysis was performed using the GeneChip Human Genome U133 Plus 2.0 Array (Affymetrix). Data normalization and gene ontology (GO) analysis were performed with GeneSpring GX software (Agilent Technologies). Gene set enrichment analysis (GSEA) (Broad Institute) and TCGA data analysis were performed on the websites <http://software.broadinstitute.org/gsea/index.jsp> and <http://www.oncolnc.org/>, respectively. The latter analysis was based on a Tier 3 mRNA dataset, which includes data for 379 gastric cancer patients (247 male and 132 female).<sup>22</sup> The gene expression data have been deposited in the Gene Expression Omnibus (GEO) (GSE139331).

## 2.6 | Single-cell analysis

Cells were isolated on C1 plates using the Biomark system (Fluidigm). Single cells were separated using a C1 Single-Cell Auto Prep Reagent Kit (Fluidigm) and C1 Single-Cell Auto Prep IFC for Preamp (10–17  $\mu$ m and 17–25  $\mu$ m) (Fluidigm). RNA was extracted and cDNA was synthesized and preamplified using an Ambion Single Cell-to-CT qRT-PCR Kit (Thermo Fisher Scientific). These cDNA were preamplified using pooled primer sets for 47 genes. Primer sequences are listed in Table S1. Products were amplified using individual primers, 48.48 Dynamic Array IFC EvaGreen (Fluidigm), GE 48.48 Dynamic Array DNA Binding Dye (Fluidigm) and SsoFast EvaGreen Supermix Low ROX (Bio-Rad). The data were analyzed using the Fluidigm Real-Time PCR Analysis software (Fluidigm). We also used program language R to analyze data in more detail using heatmap, violin plot and *t*-distributed stochastic neighbor embedding (tSNE) analyses.

## 2.7 | Small interfering RNA-mediated knockdown

Silencer Select siRNA for *LGR5*, *TROY*, *ALDH1A3*, *DKK1*, *CXCL8*, *LAMA3* and *LAMC2* were purchased from Thermo Fisher Scientific. Cells were transfected with the siRNA using RNAiMAX Transfection Reagent (Thermo Fisher Scientific). After a 2-day incubation, cells were collected and the knockdown efficiency was examined by reverse transcription-quantitative PCR (RT-qPCR) and western blot analysis, as described below.

## 2.8 | Western blot analysis

Cells were lysed in TNE lysis buffer consisting of 150 mmol/L NaCl, 0.5% Nonidet P-40, 60 mmol/L Tris and 1 mmol/L EDTA, supplemented with 1 $\times$  protease inhibitor cocktail (Nacalai Tesque) and PhosSTOP phosphatase inhibitor cocktail (Roche). Western blot analysis was performed as described previously.<sup>23</sup> Primary antibodies used in this study were as follows: mouse anti-ALDH1A3 (0.5  $\mu$ g/mL, GT926; GeneTex), rabbit anti-phospho-p70S6 kinase (p70S6K, phosphorylated at T389) (1:1000, #9234; Cell Signaling Technology), rabbit anti-p70S6K (1:1000, #9202; Cell Signaling Technology), rabbit anti-phospho-4E-BP1 (phosphorylated at S65) (1:1000, #2855; Cell Signaling Technology), rabbit anti-4E-BP1 (1:1000, #9644; Cell Signaling Technology) and mouse anti-GAPDH (0.02  $\mu$ g/mL, 10R-G109a; Fitzgerald).

## 2.9 | Vector construction and transfection

Short hairpin RNA (shRNA) sequences were designed according to the MISSION shRNA clones (Sigma-Aldrich) and the oligonucleotides were synthesized by FASMAC. Oligonucleotides were hybridized and cloned into the stuffer sites of pLKO.1 plasmid (Addgene). Lentiviruses were produced as described previously<sup>24</sup> and used to infect JSC15-3 cells. The infected cells were selected with 1  $\mu$ g/mL puromycin for 8 days. The sequences of shRNA are as follows: *ALDH1A3* #2 Fw: 5'-CCGGGCAACCAATACTGAAGTTCAACTCGAGTTGAACTTCAGTATTGGTTGCTTTTGG-3', Rv: 5'-AATTCAAAAAGCAACCAATACTGAAGTTCAACTCGAGTTGAACTTCAGTATTGGTTGCTTTTGG-3'; *ALDH1A3* #3 Fw: 5'-CCGGGCTGTATTAGAACCCTCAGATCTCGAGATCTGAGGGTTCTAATACAGCTTTTGG-3', Rv: 5'-AATTCAAAAAGCTGTATTAGAACCCTCAGATCTCGAGATCTGAGGGTTCTAATACAGC-3'.

## 2.10 | Immunohistochemistry

Tissue microarrays containing gastric cancer tissues were purchased from US Biomax. Deparaffinization and heat-induced epitope retrieval were performed as described previously.<sup>25</sup> Sections were incubated with Blocking One Histo (Nacalai Tesque) or 5  $\mu$ g/mL

mouse anti-ALDH1A3 antibody (GT926, GeneTex) at 4°C overnight. Specific signals were detected using the ChemMate Envision Kit/HRP (Agilent Technologies), and the staining intensity was scored semi-quantitatively by a pathologist (TM).

## 2.11 | Immunofluorescence staining

Immunofluorescence staining was performed as described in Nakamura (2017).<sup>25</sup> In brief, cells were fixed with 2% formaldehyde and incubated with 10 mg/mL BSA. The primary antibody was mouse anti-ALDH1A3 antibody (2 µg/mL; GT926, GeneTex).

## 2.12 | Cell cycle analysis

Quantitation of the cell cycle distribution and sub-G1 fraction was performed with flow cytometry as described previously.<sup>26</sup> In brief, cells were fixed with 70% ethanol and stained with 50 µg/mL propidium iodide. Cells were analyzed by flow cytometry with a FACSCalibur (BD Biosciences).

## 2.13 | Mouse xenograft studies

All animal procedures were performed according to the protocols approved by the JFCR Animal Care and Use Committee. Nude mice (Charles River Laboratories Japan) were subcutaneously injected with 100 µL of the cell mixture, which was prepared as  $2 \times 10^6$  cells in a 1:1 mixture of Hank's Balanced Salt Solution (Thermo Fisher Scientific) and Matrigel (Corning) of the same quantity. When the average tumor volume reached 118 mm<sup>3</sup>, the mice were divided into three groups ( $n = 3$ ) and treated with PBS or 75 or 150 mg/kg 5-FU, every 7 days. In other experiments, NOD-SCID mice (Charles River Laboratories Japan) were subcutaneously injected with 100 µL of the cell mixture, which was prepared as  $1.5 \times 10^6$  cells using a 1:1 mixture of the culture medium and Matrigel (Corning) of the same quantity. The length (L) and width (W) of the tumor were measured, and the tumor volume was calculated as  $(L \times W^2)/2$ . Measurement was performed using a digital caliper every 3 or 4 days.

# 3 | RESULTS

## 3.1 | Anticancer drugs alter the patterns of heterogeneity in the gastric cancer patient-derived cell population

To examine the alteration of gastric cancer cell populations upon treatment with anticancer drugs, we conducted single-cell analysis for the expressions of gastric tissue lineage, stem cell and drug-tolerant persister-related genes. Gastric tissue consists of cells in various differentiation stages, including stem, progenitor, surface mucous,

mucous gland and chief cells and endocrine cells, and specific markers for each cell type have been established (Figure 1A).<sup>13-19</sup> To induce persister cells, JSC15-3 cells were treated with 3 µmol/L 5-FU or 30 nmol/L SN38, an active metabolite of irinotecan, for 7 days and JSC17-2 cells were treated with 3 µmol/L 5-FU for 6 days. We focused on these two drugs because their prodrugs, capecitabine, tegafur and irinotecan, are commonly used for gastric cancer treatment in Japan. The residual persister cells showed slower growth rates and cross-resistance to 5-FU and SN38 (Figure S1A and B). RNA were prepared from persister cells and subjected to GeneChip microarray analysis. Genes upregulated more than 1.5-fold to 2-fold in persister cells compared with untreated cells were selected as persister-related genes (Figure 1B, Figure S1C,D).

We separated single cells from patient-derived gastric cancer JSC15-3 cells using the C1 Auto Prep System and examined the heterogeneity of the cell population in terms of the expression of lineage, stem and persister-related genes (Figure 1C and Table S3). Hierarchical clustering of the cells before and after 5-FU treatment revealed that most of the persister cells after 5-FU treatment were co-clustered in the same group (Figure 1C). Approximately 10% (9 of 89 cells) of untreated cells were classified into the large cluster of 5-FU-treated cells, whereas 3.3% (3 of 89 cells) of 5-FU-treated cells were in the cluster of untreated cells. Similar trends of outlier cells were also observed in tSNE plot analysis (Figure 1D). These observations indicate that most of the persister cancer cells after 5-FU treatment showed an altered gene expression signature, whereas untreated cancer cells contain a minor preexisting cell subpopulation with a similar gene expression signature to that of the persister cells.

## 3.2 | ALDH1A3 upregulation in the drug-tolerant persister cancer cells

Based on the above hierarchical clustering of the single cells (Figure 1C), we classified the cells into four categories: (a) untreated cells in the major cell clusters; (b) untreated cells in 5-FU-treated cell clusters; (c) 5-FU-treated cells in the major cell clusters; and (d) 5-FU-treated cells in untreated cell clusters. Each gene expression at the single-cell level was illustrated by violin plot analysis according to the four categories (Figure 2A and data not shown). Several genes, such as *LGR5*, *TROY*, *ALDH1A3*, *DKK1*, *CXCL8*, *LAMA3* and *LAMC2* genes, were upregulated in the 5-FU-treated cells in the major cell clusters (Figure 2A, blue). Among these genes, *ALDH1A3* gene expression was heterogeneous in cells before drug treatment (Figure 2A, red), whereas the untreated cells in 5-FU-treated cell clusters (light green) and the 5-FU-treated cells in untreated cell clusters (brown) exhibited higher and lower *ALDH1A3* gene expression, respectively, compared with those in the major cell clusters. To examine the functional significance of the genes upregulated by 5-FU in JSC15-3 cell growth and survival, we knocked down the genes by siRNA (Figure 2B and data not shown). Clonogenic assay revealed different effects of each gene knockdown on the colony-forming ability of cells (Figure 2C and data not shown). *ALDH1A3*

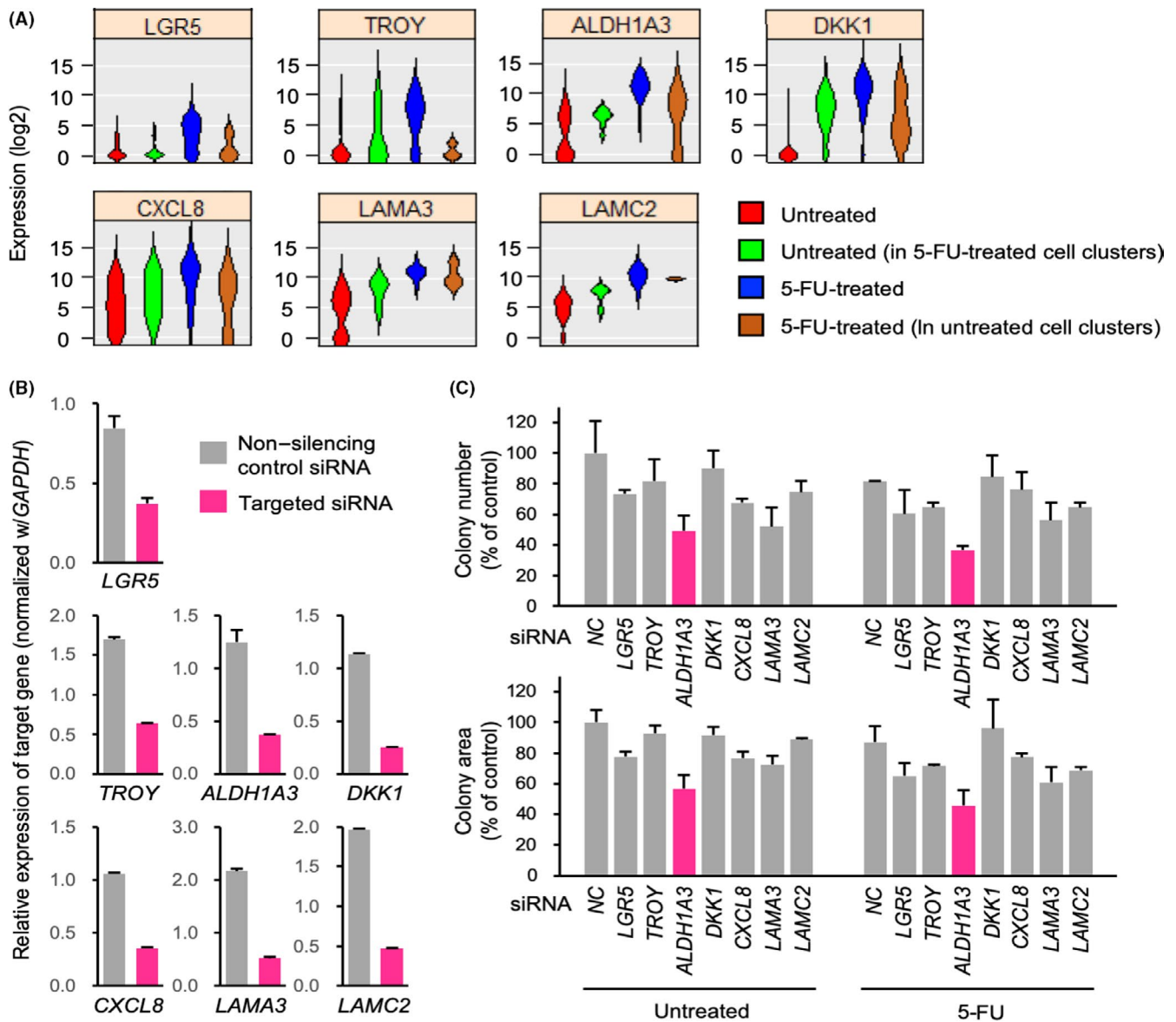


**FIGURE 2** Heterogeneous expression and 5-fluorouracil (5-FU)-induced upregulation of stem and persister-related genes and their impact on clonogenic growth of JSC15-3 cells. A, Violin plot of gene expression in gastric cancer JSC15-3 cells before and after 5-FU treatment. Cells were classified into four categories as in Figure 1C,D. B, Knockdown of genes selectively overexpressed in 5-FU-tolerant persister cells. Cells were transfected with the indicated siRNA. After a 2-day incubation, the levels of gene expression were determined by reverse transcription-quantitative PCR. C, Effect of gene knockdown on the clonogenic growth of JSC15-3 cells in the presence or absence of 1  $\mu$ mol/L 5-FU. Cells were treated as in (B) and the clonogenic growth was evaluated

knockdown showed the most potent inhibition of clonogenic growth of the cells (Figure 2C).

To examine the specificity of *ALDH1A3* upregulation among *ALDH* family members in the persister cells after 5-FU treatment, we examined the RNA levels of *ALDH* isozymes. As shown in Figure 3A and Figure S2A, *ALDH1A3* mRNA expression was commonly and selectively elevated in persister cells after 5-FU treatment in three PDC lines. Moreover, *ALDH1A3* mRNA expression was increased not only after 5-FU treatment but also after treatment with SN38, cisplatin and paclitaxel (Figure 3B and Figure S2B). The elevated *ALDH1A3* expression in persister cells was also confirmed at the protein level by immunofluorescence staining (Figure 3C). Of note,

DMSO-treated control cells exhibited heterogeneity in *ALDH1A3* staining and only portions of the cell subpopulations were *ALDH1A3*-positive. Treatment with 5-FU raised the rates of *ALDH1A3*-positive cell subpopulations, consistent with the single-cell analysis results (Figure 2A). We further monitored *ALDH1A3* expression in drug-tolerant persister cells in vivo using a mouse xenograft tumor model. As shown in Figure S3, 5-FU retarded the growth of JSC15-3-derived tumors in mice. In the residual tumor cells after drug treatment, *ALDH1A3* expression was upregulated compared with the control group treated with PBS (Figure 3D). These observations indicate that *ALDH1A3* upregulation is a common feature of persister cells after treatment with 5-FU and SN38 in gastric cancer PDC.

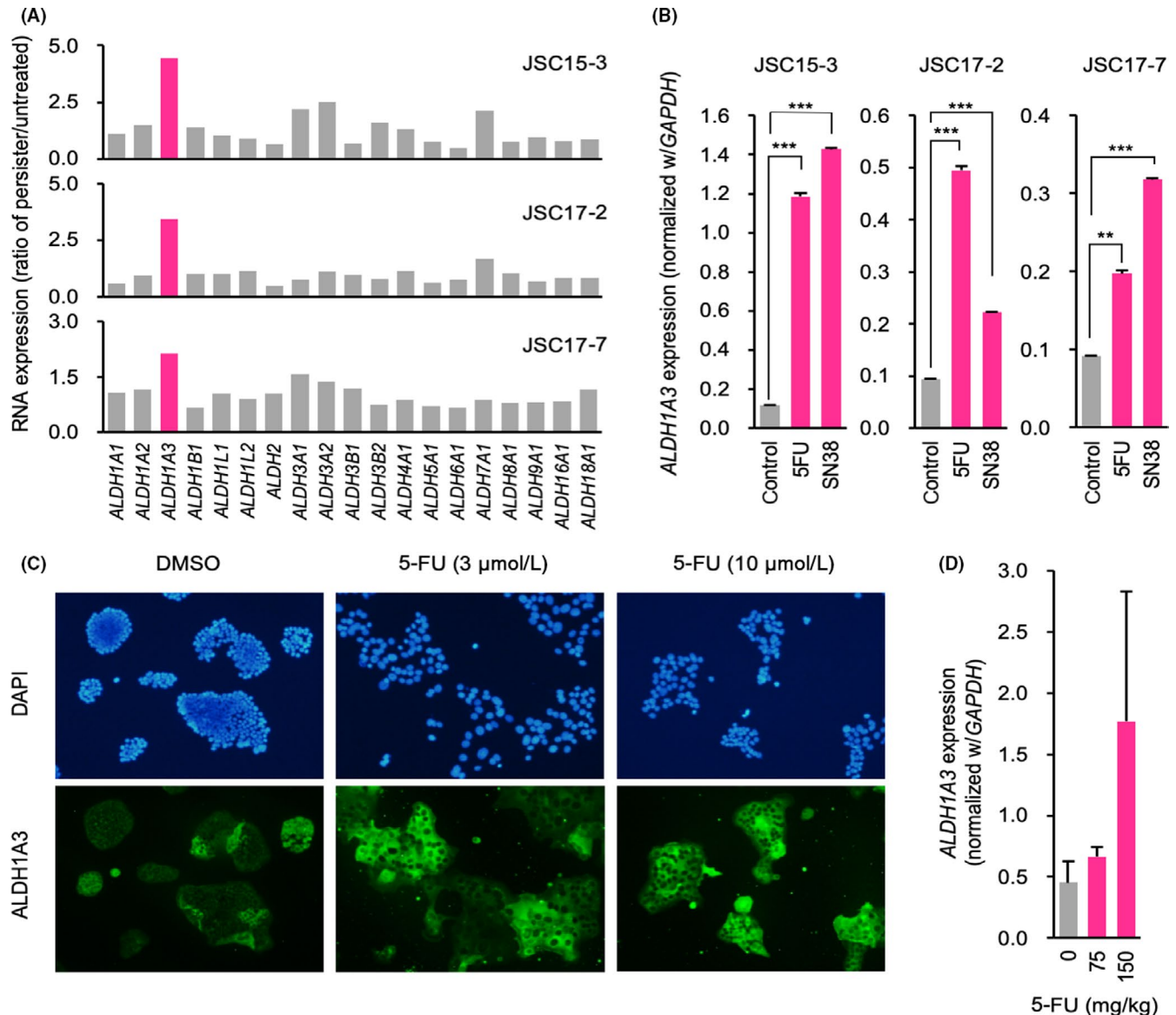


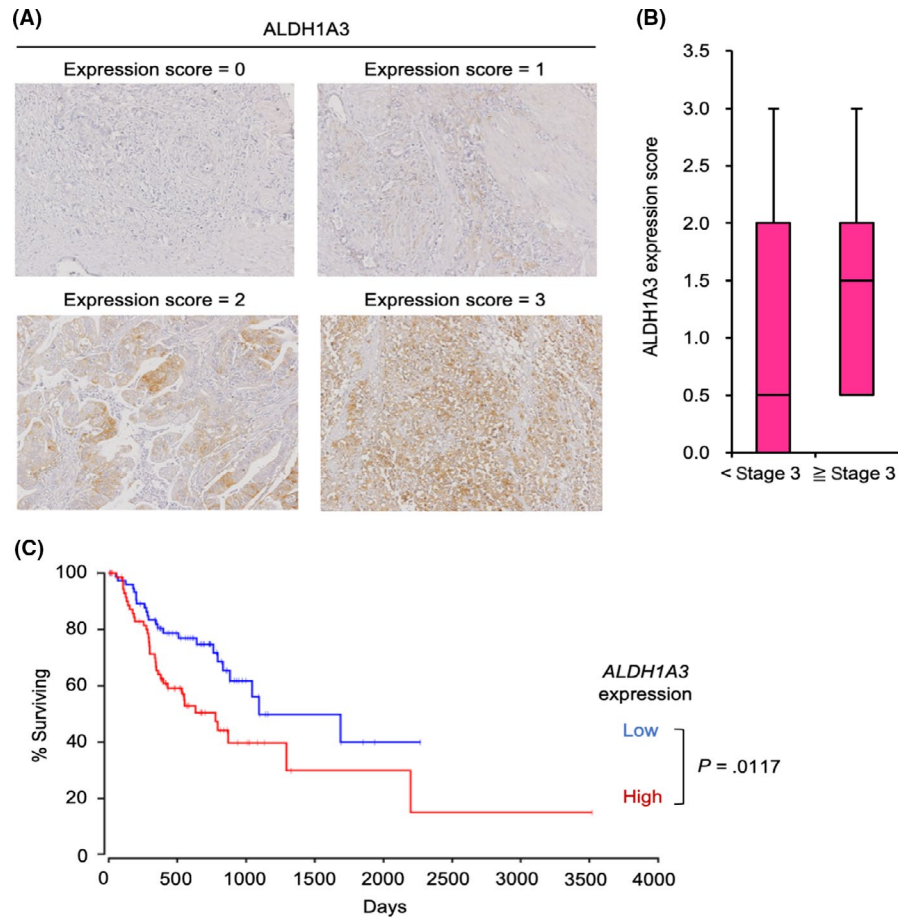
**FIGURE 3** Selective upregulation of ALDH1A3 in gastric cancer patient-derived cells after treatment with cytotoxic anticancer drugs. A, mRNA expression of ALDH family members in gastric cancer patient-derived cells after 5-fluorouracil (5-FU) treatment. Cells were treated with 3 μmol/L (JSC15-3 and JSC17-2) or 1 μmol/L (JSC17-7) of 5-FU for 7 days (JSC15-3) or 6 days (JSC17-2 and JSC17-7), and the expression levels of the indicated genes were determined by GeneChip microarray analysis. The vertical axis indicates the fold change upregulation in 5-FU-treated cells compared with untreated cells. B, mRNA expression of ALDH1A3 in gastric cancer patient-derived cells after treatment with anticancer drugs. Cells were treated with 10 μmol/L (JSC15-3), 3 μmol/L (JSC17-2) or 0.3 μmol/L (JSC17-7) of 5-FU or 100 nmol/L (JSC15-3) or 10 nmol/L (JSC17-2 and SC17-7) of SN38 for 7 days (JSC15-3) or 6 days (JSC17-2 and JSC17-7). ALDH1A3 mRNA levels were quantitated by reverse transcription-quantitative PCR (RT-qPCR). \*\* $P < .01$ , \*\*\* $P < .001$ . C, Immunofluorescence staining. JSC15-3 cells were treated with 5-FU for 6 days and subjected to indirect immunofluorescence staining. DNA was counterstained with DAPI. D, Effect of 5-FU on ALDH1A3 expression in JSC15-3 xenograft tumors. Nude mice with JSC15-3-derived tumors were treated with 5-FU. RNA was prepared and subjected to RT-qPCR

### 3.3 | ALDH1A3 expression correlates with advanced stage and poor prognosis of gastric cancer

We have so far demonstrated that ALDH1A3 is required for clonogenic growth of gastric cancer PDC and is upregulated in the drug-tolerant persister fraction of PDC. We next monitored ALDH1A3 expression in patient-derived gastric tumors using tissue microarrays. Immunohistochemical analysis was performed on the

microarrays, and the sections were scored according to the level of ALDH1A3 expression (Figure 4A and Figure S4). We observed a trend that ALDH1A3 expression was higher in advanced gastric tumors later than stage 3 (Figure 4B), although the difference was not statistically significant ( $P = .27$ ). Furthermore, TCGA database analysis revealed that the patients in the highest fifth of ALDH1A3 expression showed poorer prognosis than those in the lowest fifth (Figure 4C). These observations suggest that ALDH1A3 expression

**FIGURE 4** ALDH1A3 is a poor prognostic factor of gastric cancer. A, Immunohistochemistry of gastric cancer tissue microarray. ALDH1A3 protein was detected by immunohistochemistry, and the tissue samples were classified into four categories according to the signal intensities (expression scores of 0 to 3). Representative samples from each category are shown. B, Comparison of ALDH1A3 expression score between cancer tissues earlier than stage 3 and later than stage 3. C, Kaplan-Meier curves for overall survival of gastric cancer patients with high or low ALDH1A3 expression. Curves were drawn according to the data in the TCGA public database



is associated with advanced stage and poor prognosis of gastric cancer.

### 3.4 | ALDH1A3 facilitates the growth and survival of gastric cancer patient-derived cells and drug-tolerant persister cells

To examine the functional role of ALDH1A3 in gastric cancer cells that persist after 5-FU or SN38 treatment, we constitutively knocked down ALDH1A3 in JSC15-3 cells using two different short hairpin RNA (shRNA #2 and #3) (Figure 5A). Consistent with our results above, ALDH1A3 knockdown inhibited the growth of JSC15-3 cells not exposed to 5-FU and SN38 (Figure 5B,C). Furthermore, the residual cell numbers were reduced among ALDH1A3-depleted cells in response to 5-FU and SN38 compared with control cells; however, we did not observe synergistic but additive effects of ALDH1A3 knockdown and 5-FU/SN38 treatment. Consistent with these observations, flow cytometry analysis revealed that the ALDH1A3-depleted JSC15-3 cells showed higher rates of sub-G1 apoptotic cell fractions compared with control cells upon treatment with 5-FU (Figure S5). To validate the role of ALDH1A3 in tumor growth in vivo, we subcutaneously injected mock and ALDH1A3-depleted JSC15-3 cells into NOD-SCID mice (mock:  $n = 7$ ; ALDH1A3-depleted:  $n = 8$ ). The rates of tumor formation were 100% and 50% in the mock and

ALDH1A3-depleted cell groups, respectively. Furthermore, the tumor size was significantly reduced ( $P < .001$ ) in the ALDH1A3-depleted cell group (Figure 5D). These observations indicate that ALDH1A3 contributes to the growth and survival of gastric cancer PDC and drug-tolerant persister cells.

### 3.5 | ALDH1A3 depletion downregulates the mammalian target of rapamycin pathway in gastric cancer patient-derived cells

To clarify how ALDH1A3 regulates gastric cancer PDC survival, we next performed comprehensive transcriptome analysis on JSC15-3 control (parental and non-silencing shRNA) and ALDH1A3 knockdown (shRNA #2 and #3) cells (Figure S6A). Gene ontology analysis revealed that ALDH1A3 knockdown affected cell cycle-related genes (Table S4). GSEA revealed that the expressions of genes associated with mTOR and MEK pathways were altered in ALDH1A3-depleted cells (Figure 6A and Figure S6B). In particular, the genes upregulated by an mTOR inhibitor, everolimus (MTOR\_UP.V1\_UP; systematic name: M2672), were enriched in the gene set highly expressed in ALDH1A3-depleted cells. In addition, genes downregulated by everolimus (MTOR\_UP.V1\_DN; systematic name: M2670) were enriched in the gene set that was poorly expressed in ALDH1A3-depleted cells (Figure 6A). Thus, the mTOR pathway



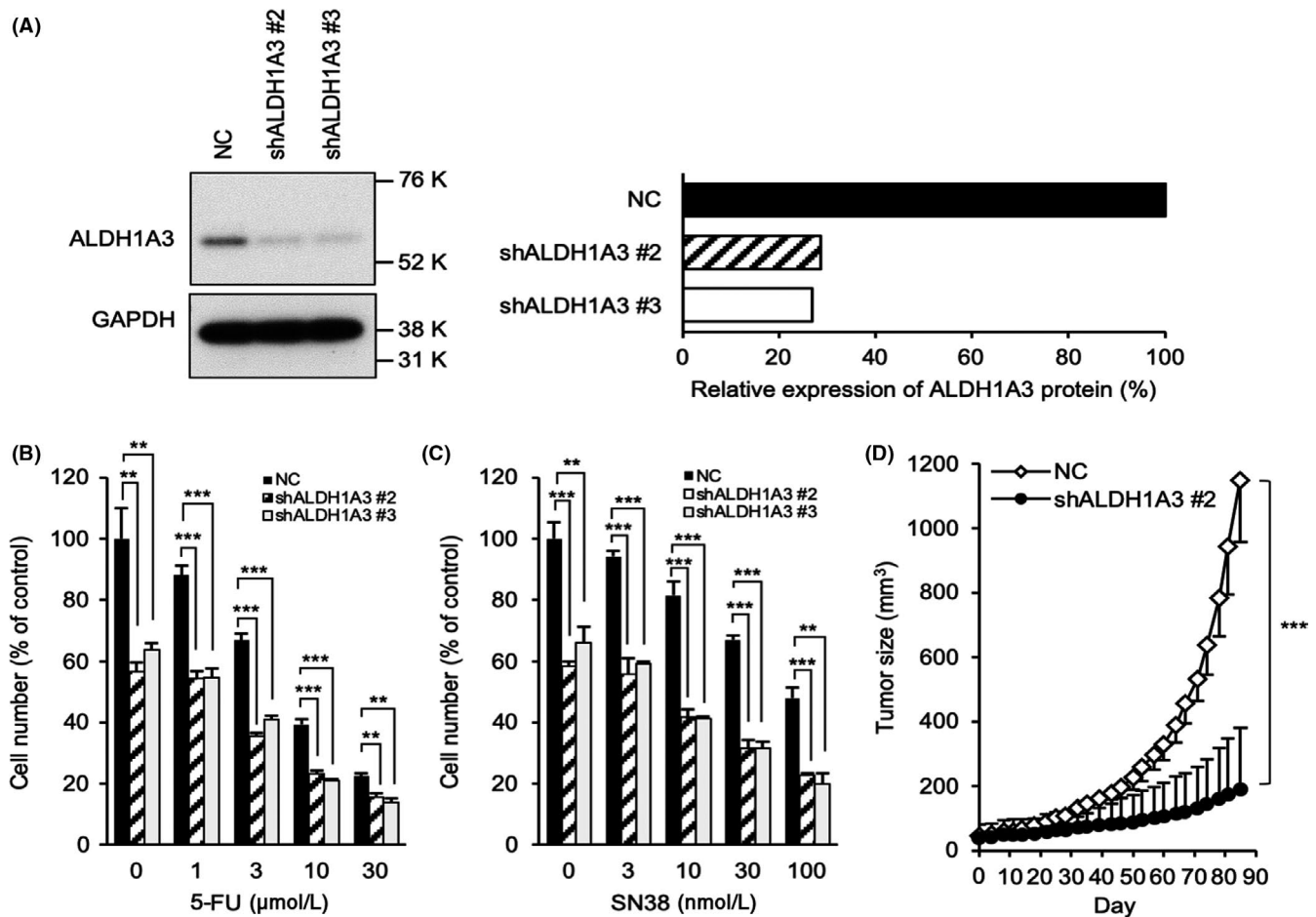


**FIGURE 5** ALDH1A3 depletion decreases the cell viability and number of the drug-tolerant persister cells in gastric cancer patient-derived cells. A, ALDH1A3 knockdown in JSC15-3 cells. Cells that constitutively express ALDH1A3 shRNA or non-silencing control shRNA (NC) were subjected to western blot analysis (left). A quantitative graph is shown (right). B, C, Effect of ALDH1A3 knockdown on the drug-tolerant cells. Cells transfected as in (A) were treated with 5-FU (B) or SN38 (C) for 7 days, and the cell numbers were quantitated. D, In vivo tumor growth of ALDH1A3-depleted JSC15-3 cells. NOD-SCID mice were subcutaneously injected with the cells transfected as in (A). Tumor growth was evaluated as described in the Materials and Methods. \*\* $P < .01$ , \*\*\* $P < .001$

was commonly extracted from both directions of GSEA. Consistent with these observations, the ALDH1A3-depleted cells showed a reduced level of activating phosphorylation of p70 S6 kinase, one of the downstream effectors of the mTOR pathway (Figure 6B,C). To validate the functional involvement of the mTOR pathway in the cell growth and survival, we treated cells with temsirolimus, a specific mTOR inhibitor, in the absence or the presence of 5-FU. As shown in Figure 6D, the combination of temsirolimus and 5-FU reduced the number of persister cells compared with either temsirolimus or 5-FU. These observations indicate that the mTOR pathway may be involved in gastric cancer persister cell maintenance downstream of ALDH1A3.

## 4 | DISCUSSION

In the present study, we found that drug-tolerant gastric cancer persister cells express multiple stem or cancer stem cell markers, including *LGR5* and *TROY*. These observations suggest that the early phase

of anticancer drug resistance could be linked to stemness of persister cells. We observed that stem cell marker-expressing persister cells were slow growing (Figure S1A). This stem-like “dormant” characteristic of the persister cells may be linked with drug resistance.

Although the residual cancer cells after 5-FU treatment expressed multiple stem cell markers, the expression patterns of the markers were not necessarily uniform (Figure 2A). Compared with other stem cell markers, such as *LGR5* and *TROY*, *ALDH1A3* expression was more heterogeneous in the untreated cell population and upregulated to more uniform and higher levels in the drug-tolerant persister cells (Figure 2A). Notably, although *TROY* is involved in resistance to radiotherapy and chemotherapy in glioblastoma,<sup>27</sup> the drug-tolerant persister cells in this study showed *TROY*-negative and low-expressing cell fractions (Figure 2A). These observations suggest that *ALDH1A3* may be a better marker for persister cells than other stem cell-related factors. In fact, *ALDH1A3* expression was commonly upregulated in multiple drug-tolerant persister cells, including those treated with 5-FU, SN38, cisplatin and paclitaxel. To support this notion, the prognostic analysis based on the TCGA

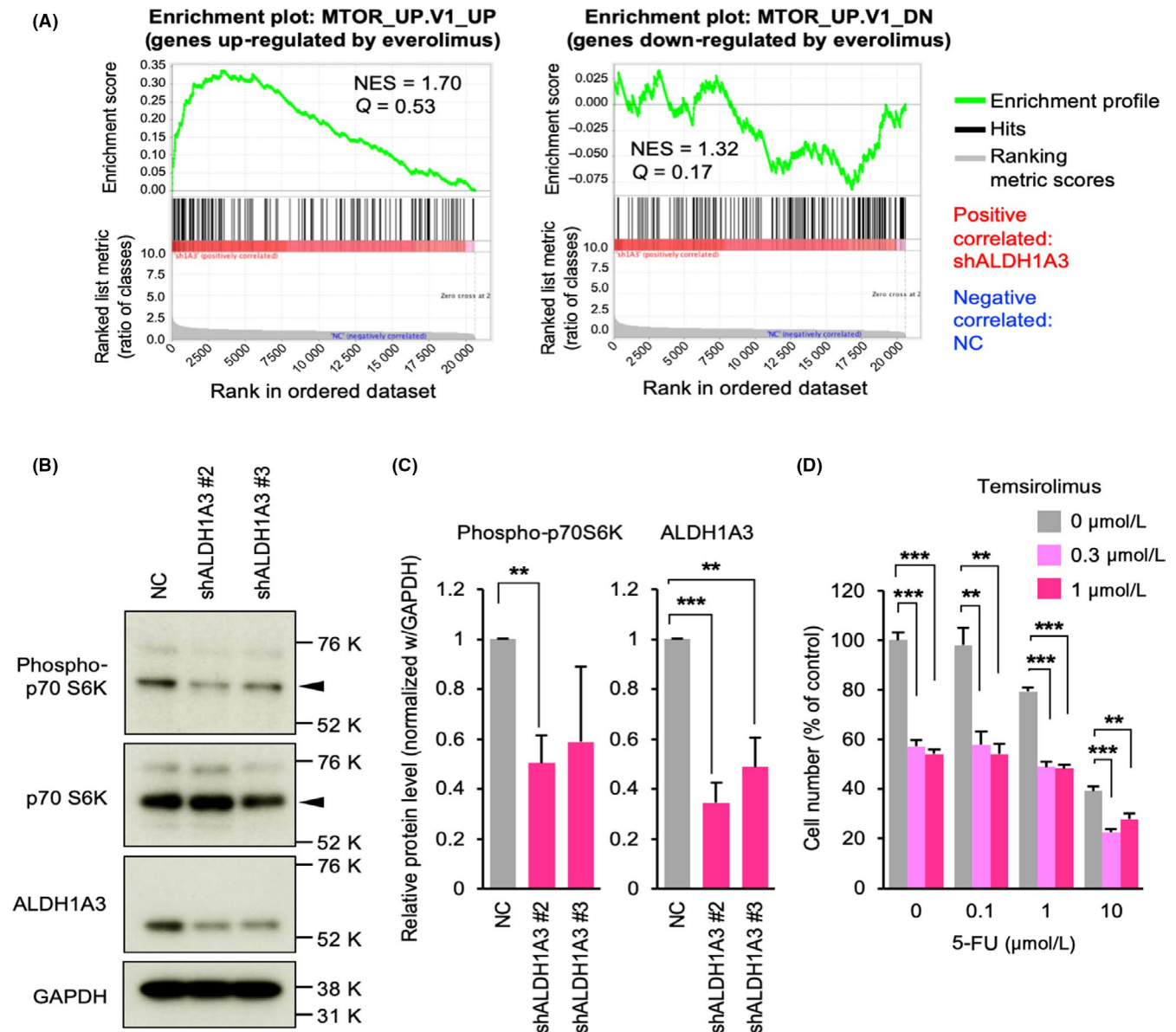


**FIGURE 6** Involvement of the mammalian target of rapamycin (mTOR) pathway in ALDH1A3-mediated drug tolerance of gastric cancer patient-derived cells. A, Gene set enrichment profiles of ALDH1A3-depleted JSC15-3 cells. Transcriptome data were analyzed by gene set enrichment analysis (GSEA), which identified the upregulated and downregulated gene sets by everolimus. B, Western blot analysis of ALDH1A3-depleted JSC15-3 cells. C, Quantitative representation of protein levels shown in (B). The experiments were repeated three times and the graph indicates the average and standard deviation. D, Effect of temsirolimus on 5-FU-tolerant JSC15-3 cells. Cells were treated with the indicated concentrations of 5-fluorouracil (5-FU) for 7 days, and the cell numbers were quantitated. \*\* $P < .01$ , \*\*\* $P < .001$

database showed that *ALDH1A3* expression is associated with poor prognosis of gastric cancer patients (Figure 4C).

Thus far, how *ALDH1A3* expression is specifically upregulated among the *ALDH* isozymes in the gastric cancer drug-tolerant persister cells is unclear. Feng et al<sup>28</sup> reported that *ALDH1A3* is the major isozyme that contributes to *ALDH* enzyme activities in 58 human cancer cell lines. In breast cancer, glioma and melanoma, *ALDH1A3* expression is regulated by several mechanisms at epigenetic, transcriptional and posttranslational levels.<sup>29-31</sup> For example, *ALDH1A3* is upregulated at the transcriptional level by *FOXD1* in mesenchymal glioma stem cells (MES GCS).<sup>30</sup> *FOXD1* expression is positively associated with *ALDH1A3* expression but not with

expressions of other *ALDH* members in MES GCS.<sup>30</sup> Another study showed that *ALDH1A3* is ubiquitinated by the ubiquitin-specific protease 9X (*USP9X*) and stabilized in MES GCS, although the *USP9X* preference for *ALDH1A3* among many *ALDH* isozymes has not been addressed.<sup>32</sup> Because *ALDH1A3* upregulation was observed at the mRNA level in persister cells (Figure 3A), specific transcription factors other than *FOXD1*, which is overexpressed in brain but not gastric cancer (Oncomine database), may be involved in *ALDH1A3* gene upregulation.

*ALDH1A3* has recently been shown to play a pivotal role in mesenchymal glioma stem cell maintenance and colorectal cancer proliferation,<sup>28,32</sup> whereas its role in gastric cancer tumorigenesis and

malignancy is not clear. Here we showed that ALDH1A3 is not only a marker of persister cells after treatment with cytotoxic anticancer drugs but is also involved in the cell survival and tumor-initiating and propagating activities of gastric cancer cells. Because ALDH1A3 knockdown led to an increase in the apoptotic sub-G1 cell fraction upon treatment with 5-FU (Figure S5), it is likely that ALDH1A3 supports the survival of gastric cancer persister cells. Moreover, our gene ontology analysis showed that ALDH1A3 knockdown affected cell cycle-related pathways (Table S4), suggesting that ALDH1A3 may also be involved in cell cycle regulation and dormancy of persister cells.

As the downstream mediator of ALDH1A3, we focused on the mTOR pathway because it is involved in cancer cell survival and proliferation, and there are clinically approved inhibitors of this pathway. In a clinical setting, a recent phase III study revealed that everolimus did not improve the therapeutic outcome of paclitaxel in advanced gastric cancer. Intriguingly, however, everolimus improved the progression-free survival and overall survival of the patient subgroup who received prior taxane therapy.<sup>33</sup> Moreover, there was a phase II study that demonstrated effectiveness of capecitabine and everolimus combination in a small subset of refractory gastric cancer patients.<sup>34</sup> We observed inter-tumor and intra-tumor heterogeneity of ALDH1A3 expression in gastric cancer cells and tissues (Figures 2-4 and Figure S4). These observations suggest that the contribution of the ALDH1A3-mTOR axis to cell survival and proliferation may be restricted to a subset of gastric cancer. This could explain why mTOR-targeted therapies were effective only in a small subset of the patients. It would be important to identify the biomarkers that predict the outcome of the combination therapies.

Our GSEA results further suggest a relationship between ALDH1A3 and other cell signaling pathways, such as MAPK pathways (Figure S6). Xie et al (2019) report that the matricellular proteins TNC1 and ESM1 mediate the pro-proliferative function of ALDH1A3 through activation of AKT/mTOR and/or MEK/ERK pathways in smooth muscle cells.<sup>35</sup> In our patient-derived gastric cancer cells, however, the basal RNA expression levels of TNC1 and ESM1 were too low for detection by GeneChip microarray and RT-qPCR, and neither 5-FU nor SN38 induced these gene expression (RK, TM and HS, unpublished observations). These observations suggest that TNC1 and ESM1 do not mediate the ALDH1A3-dependent cell proliferation at least in our gastric cancer cell models.

In summary, our single-cell gene expression analysis and subsequent functional analyses identified ALDH1A3 as a key survival factor of drug-tolerant persister cells in gastric cancer. ALDH1A3-targeting therapy in combination with standard chemotherapy may represent a novel therapeutic strategy in gastric cancer to overcome tumor recurrence.

## ACKNOWLEDGMENTS

We would like to thank members of the Seimiya laboratory for invaluable discussion. This work was supported in part by Japan Society for the Promotion of Science (JSPS) KAKENHI grants (number 18H04633 to HS and 18K07337 to TM) and a research grant from The Nippon Foundation to HS. Funding for open access charge:

Japan Society for the Promotion of Science/18H04633. We thank Edanz Group ([www.edanzediting.com/ac](http://www.edanzediting.com/ac)) for editing a draft of this manuscript.

## CONFLICT OF INTEREST

Competing interests: HS received a research grant from The Nippon Foundation. The other authors have no competing interests to disclose.

## ORCID

Hiroyuki Seimiya  <https://orcid.org/0000-0003-3314-9736>

## REFERENCES

- Rahman R, Asombang AW, Ibdah JA. Characteristics of gastric cancer in Asia. *World J Gastroenterol*. 2014;20:4483-4490.
- Nowell PC. The clonal evolution of tumor cell populations. *Science*. 1976;194:23-28.
- Magee JA, Piskounova E, Morrison SJ. Cancer stem cells: impact, heterogeneity, and uncertainty. *Cancer Cell*. 2012;21:283-296.
- Sharma SV, Lee DY, Li B, et al. A chromatin-mediated reversible drug-tolerant state in cancer cell subpopulations. *Cell*. 2010;141:69-80.
- Hangauer MJ, Viswanathan VS, Ryan MJ, et al. Drug-tolerant persister cancer cells are vulnerable to GPX4 inhibition. *Nature*. 2017;551:247-250.
- Al-Hajj M, Wicha MS, Benito-Hernandez A, et al. Prospective identification of tumorigenic breast cancer cells. *Proc Natl Acad Sci USA*. 2003;100:3983-3988.
- Singh SK, Hawkins C, Clarke ID, et al. Identification of human brain tumour initiating cells. *Nature*. 2004;432:396-401.
- O'Brien CA, Pollett A, Gallinger S, et al. A human colon cancer cell capable of initiating tumour growth in immunodeficient mice. *Nature*. 2007;445:106-110.
- Takaishi S, Okumura T, Tu S, et al. Identification of gastric cancer stem cells using the cell surface marker CD44. *Stem Cells*. 2009;27:1006-1020.
- Lau WM, Teng E, Chong HS, et al. CD44v8-10 is a cancer-specific marker for gastric cancer stem cells. *Cancer Res*. 2014;74:2630-2641.
- Ishimoto T, Nagano O, Yae T, et al. CD44 variant regulates redox status in cancer cells by stabilizing the xCT subunit of system xc(-) and thereby promotes tumor growth. *Cancer Cell*. 2011;19:387-400.
- Mashima T, Iwasaki R, Kawata N, et al. In silico chemical screening identifies epidermal growth factor receptor as a therapeutic target of drug-tolerant CD44v9-positive gastric cancer cells. *Br J Cancer*. 2019;121:846-856.
- Lee ER, Trasler J, Dwivedi S, et al. Division of the mouse gastric mucosa into zymogenic and mucous regions on the basis of gland features. *Am J Anat*. 1982;164:187-207.
- McCracken KW, Catá EM, Crawford CM, et al. Modelling human development and disease in pluripotent stem-cell-derived gastric organoids. *Nature*. 2014;516:400-404.
- Barker N, Huch M, Kujala P, et al. Lgr5(+ve) stem cells drive self-renewal in the stomach and build long-lived gastric units in vitro. *Cell Stem Cell*. 2010;6:25-36.
- Choi E, Roland JT, Barlow BJ, et al. Cell lineage distribution atlas of the human stomach reveals heterogeneous gland populations in the gastric antrum. *Gut*. 2014;63:1711-1720.
- Hoffmann W. Current status on stem cells and cancers of the gastric epithelium. *Int J Mol Sci*. 2015;16:19153-19169.
- Leushacke M, Tan SH, Wong A, et al. Lgr5-expressing chief cells drive epithelial regeneration and cancer in the oxyntic stomach. *Nat Cell Biol*. 2017;19:774-786.

19. Huang Q, Zou X. Clinicopathology of early gastric carcinoma: an update for pathologists and gastroenterologists. *Gastrointest Tumors*. 2017;3:115-124.
20. Chung W, Eum HH, Lee HO, et al. Single-cell RNA-seq enables comprehensive tumour and immune cell profiling in primary breast cancer. *Nat Commun*. 2017;8:15081.
21. Prieto-Vila M, Usuba W, Takahashi RU, et al. Single-cell analysis reveals a preexisting drug-resistant subpopulation in the luminal breast cancer subtype. *Cancer Res*. 2019;79:4412-4425.
22. Anaya J. OncoLnc: linking TCGA survival data to mRNAs, miRNAs, and lncRNAs. *PeerJ Comput Sci*. 2016;2:e67. <https://doi.org/10.7717/peerj-cs.67>.
23. Mizutani A, Yashiroda Y, Muramatsu Y, et al. RK-287107, a potent and specific tankyrase inhibitor, blocks colorectal cancer cell growth in a preclinical model. *Cancer Sci*. 2018;109:4003-4014.
24. Mashima T, Soma-Nagae T, Migita T, et al. TRIB1 supports prostate tumorigenesis and tumor-propagating cell survival by regulation of endoplasmic reticulum chaperone expression. *Cancer Res*. 2014;74:4888-4897.
25. Nakamura T, Okabe S, Yoshida H, et al. Targeting glioma stem cells in vivo by a G-quadruplex-stabilizing synthetic macrocyclic hexaoxazole. *Sci Rep*. 2017;7:3605.
26. Seimiya H, Muramatsu Y, Ohishi T, et al. Tankyrase 1 as a target for telomere-directed molecular cancer therapeutics. *Cancer Cell*. 2005;7:25-37.
27. Loftus JC, Dhruv H, Tuncali S, et al. TROY (TNFRSF19) promotes glioblastoma survival signaling and therapeutic resistance. *Mol Cancer Res*. 2013;11:865-874.
28. Feng H, Liu Y, Bian X, et al. ALDH1A3 affects colon cancer in vitro proliferation and invasion depending on CXCR4 status. *Br J Cancer*. 2018;118:224-232.
29. Marcato P, Dean CA, Pan D, et al. Aldehyde dehydrogenase activity of breast cancer stem cells is primarily due to isoform ALDH1A3 and its expression is predictive of metastasis. *Stem Cells*. 2011;29:32-45.
30. Cheng P, Wang J, Waghmare I, et al. FOXD1-ALDH1A3 signaling is a determinant for the self-renewal and tumorigenicity of mesenchymal glioma stem cells. *Cancer Res*. 2016;76:7219-7230.
31. Pérez-Alea M, McGrail K, Sánchez-Redondo S, et al. ALDH1A3 is epigenetically regulated during melanocyte transformation and is a target for melanoma treatment. *Oncogene*. 2017;36:5695-5708.
32. Chen Z, Wang HW, Wang S, et al. USP9X deubiquitinates ALDH1A3 and maintains mesenchymal identity in glioblastoma stem cells. *J Clin Invest*. 2019;129:2043-2055.
33. Lorenzen S, Riera Knorrnschild J, Pauligk C, et al. A randomized, double-blind, multi-center phase III study evaluating paclitaxel with and without RAD001 in patients with gastric or esophagogastric junction carcinoma who have progressed after therapy with a fluoropyrimidine/platinum-containing regimen (RADPAC). *J Clin Oncol*. 2017;35(15 Suppl):4027-4027.
34. Lee SJ, Lee J, Lee J, et al. Phase II trial of capecitabine and everolimus (RAD001) combination in refractory gastric cancer patients. *Invest New Drugs*. 2013;31:1580-1586.
35. Xie X, Urabe G, Marcho L, et al. ALDH1A3 regulations of matrix-cellular proteins promote vascular smooth muscle cell proliferation. *iScience*. 2019;19:872-882.

#### SUPPORTING INFORMATION

Additional supporting information may be found online in the Supporting Information section.

**How to cite this article:** Kawakami R, Mashima T, Kawata N, et al. ALDH1A3-mTOR axis as a therapeutic target for anticancer drug-tolerant persister cells in gastric cancer. *Cancer Sci*. 2020;111:962-973. <https://doi.org/10.1111/cas.14316>